Combining hydrologic simulations and stream-network models to unveil flow-ecology relationships in a large Alpine catchment

Stefano Larsen[1,2]; Bruno Majone[2]; Patrick Zulian[2]; Elisa Stella[3]; Alberto Bellin[2]; Maria Cristina Bruno[1]; Guido Zolezzi[2].

1 Research and Innovation Centre, Fondazione Edmund Mach, via E. Mach 1, 38010 San Michele all'Adige, Italy.

2 Department of Civil, Environmental and Mechanical Engineering, University of Trento, via Mesiano 77, 38123 Trento, Italy.

3 Institute of Polar Sciences - Consiglio Nazionale delle Ricerche, Via Torino, 155, 30172, Mestre-Venice, Italy.

Key points

- The process based HYPERstreamHS hydrologic model was used to simulate natural streamflow series in 100 bio-assessment sites across a large Alpine basin.

- Three flow-regime classes were identified, representing typical nivo-glacial, nivo-pluvial, and pluvial streams.

- Spatial stream-network models identified distinct flow-ecology relationships across classified regimes, which aid implementating of tageted water management schemes.

62

Abstract

63

64

65 Flow regimes profoundly influence river organisms and ecosystem functions, but regulatory
66 approaches often lack the scientific basis to support sustainable water allocation. In part, this
67 reflects the challenge of understanding the ecological effects of flow variability over different
68 temporal and spatial extents.

69

70 Here, we use a process-based hydrologic model to simulate 23 years of natural flow regime in
71 100 reference bioassessment sites across the Adige River network (NE Italy), also identifying
72 typical nivo-glacial, nivo-pluvial, and pluvial reaches. We then applied stream-network
73 models to investigate the relationships between hydrologic and macroinvertebrate metrics
74 while accounting for network spatial autocorrelation and local habitat conditions.

75

76 Macroinvertebrate metrics correlated most strongly with maximum, minimum and temporal
77 variation in streamflow, but apparent effects varied across flow regime types. For example:
78 i) taxon richness declined with maximum streamflow in nivo-glacial streams, but increased in
79 the pluvial ones; ii) invertebrate grazers increased proportionately with flow variation in
80 nivo-glacial streams but declined in pluvial streams. Spatial Stream Network models
81 revealed that most variation in macroinvertebrate metrics was associated with spatial patterns,
82 although local land-use and water quality also affected benthic invertebrate communities,
83 particularly at lower elevations,

84

85 These findings highlight the importance of developing ecological flows in ways that reflect
86 specific hydro-ecological and land use contexts. Our data also illustrate the importance of
87 spatially explicit approaches that account for auto-correlation when quantifying flow-ecology
88 relationships.

89

90

93

94

1. Introduction

The flow regime of streams and rivers has been modified by human activities at the global scale (Grill et al., 2019; Tonkin et al., 2019). As human population continues to grow, the increasing demand for water supply, flood protection and energy production has prompted a bloom in engineering solutions such as the construction of hydroelectric dams, levees and other hydraulic infrastructures (Couto & Olden, 2018; Shumilova et al., 2018; Zarfl et al., 2015). As a result, streams and rivers are under increasing anthropogenic pressure and are among the most threatened ecosystems worldwide, with particularly high rates of species extinctions (Tickner et al., 2020). The ongoing global climate change is expected to further exacerbate this situation by increasing the frequency of extreme hydrologic events such as floods and droughts that act synergistically with other stressors affecting aquatic ecosystems, (e.g. Navarro-Ortega et al., 2015). This is of particular concern since freshwater ecosystems support about 10% of all known species (Strayer & Dudgeon, 2010) and are essential for human well-being (Green et al., 2015). Understanding and limiting the ecological effects of flow alteration is therefore fundamental for a sustainable use of water resources.

The Natural Flow Regime Paradigm (Poff et al. 1997), is at the heart of environmental flow definition and specifically acknowledges that river biota is adapted to seasonal and interannual variations of river flow. In order to mitigate the ecological impacts associated with human infrastructures while maintaining their functioning, environmental flows (termed *e-flows* hereafter) should mimic the natural streamflow variability in terms of magnitude, frequency, duration, timing and rate of change (Arthington et al., 2018). However, *e-flows* policy must be informed by a clear understanding of the relation between river ecology and flow characteristics (i.e., flow-ecology relationships), which is, however, hampered by several practical challenges. These include, among others: i) the paucity of stream and river locations for which ecological information can be paired with long term hydrologic records (e.g. Patrick & Yuan, 2017a); ii) the natural variation in flow regime among rivers and sub-catchments, whereby ecological responses could vary significantly among individual flow regime types (Poff et al., 2010); and iii) the spatial configuration of river ecosystems, which requires statistical approaches able to account for the complex autocorrelation associated with network topology and flow directionality (Peterson et al., 2013).

127   Several approaches have been used to address these challenges. Matching flow and
128   ecological data is a prerequisite for quantifying flow-ecology relationships, and yet the spatial
129   and temporal overlap between observed hydrologic and biological data is often poor (e.g.
130   Mazor et al., 2018). To alleviate such limitations, either statistical or process-based
131   hydrologic models have been used. Statistical models aim to predict hydrologic variables at
132   ungauged locations from the observed relation between available streamflow series and
133   catchment characteristics (Booker et al., 2015; Patrick & Yuan, 2017b) or by means of
134   geostatistical interpolation (Skøien et al., 2006). Process-based hydrologic models, on the
135   other hand, directly simulate streamflow time series at specific network locations by
136   integrating the hydrological processes acting within the drainage area: i.e., precipitation,
137   snowmelt, interception, evapotranspiration, infiltration, surface and sub-surface flow, as well
138   as their interaction (Beven, 2012).
139   The second challenge is related to the heterogeneity of river basins where the natural
140   streamflow regime and river biota differ markedly across the network. Therefore, it is
141   necessary to classify flow regimes into distinct and easily interpretable classes in order to
142   define reference flow conditions and implement targeted *e-flows* schemes, while also
143   minimising the effects of other co-varying environmental factors (Belmar et al., 2011; Booker
144   et al., 2015). As a result, *e-flows* could be transferred among similar flow regimes at regional
145   scales. The identification and classification of reference hydrographs are two key steps (i.e,
146   "Hydrological foundation" and "River classification") in the assessment of the "Ecological
147   Limits of Hydrologic Alteration" (ELOHA), the holistic framework increasingly adopted to
148   define regional flow standards (Poff et al., 2010).
149   The third challenge is not strictly associated with flow-ecology research, but it is related to
150   the spatial structure of river networks. The unique topology of branching river networks
151   implies that classical statistical methods are unable to account for the spatial autocorrelation
152   due to the connectivity and directionality of water flow within the network. Failing to account
153   for such spatial patterns may lead to spurious correlations (Isaak et al., 2014). However,
154   recent advances in the field of fluvial variography (i.e. spatial statistics applied to river
155   networks) have provided the tools to model these spatial dependencies over the Euclidean
156   and watercourse dimension, while also accounting for flow directionality (Carrara et al.,
157   2012; Ver Hoef & Peterson, 2010; Zimmerman & Ver Hoef, 2017). Such stream-network
158   models have been used to derive spatially-explicit estimates of water quality and population
159   abundance across river basins (Isaak et al., 2017; McGuire et al., 2014), but applications to
160   flow-ecology research are surprisingly scarce (Bruckerhoff et al., 2019).

In this paper, we contribute to the understanding of flow-ecology relationships by addressing these challenges using the Adige River basin (Northern-eastern Italy) as case study. Specifically, we focused on benthic macroinvertebrates as model organisms because of their essential role in the functioning of lotic systems, their widespread use as biological indicators and the availability of monitoring data in the region (De Pauw et al., 2006; Friberg, 2014; Larsen et al., 2019). First, we used the process-based HYPERstreamHS hydrologic model (Avesani et al., 2020) to simulate natural streamflow series in one-hundred stream reaches throughout the Adige River basin where biological information was available. Then, we classify three distinct flow regimes representing the natural hydrologic conditions of the streams in the basin. Subsequently, we used spatial stream-network models (SSN) to relate macroinvertebrate taxonomic and functional metrics with streamflow characteristics and habitat conditions within each flow regime, while also accounting for spatial autocorrelation. The use of functional metrics based on species life-history traits (e.g. feeding habits, body sizes) provides information that is independent of taxonomy, and thus allows identifying flow-ecology relationships that could be valid across biogeographic zones (Heino et al., 2013).

The study has an important relevance also at the regional scale, since recent works conducted in the Italian Alps showed the poor sensitivity of current Water Framework Directive (WFD) biological indicators to flow parameters (Larsen et al., 2019; Quadroni et al., 2017).

2. Data and Methods

2.1 Study area

The study area is the Adige River basin, an Alpine watershed in North-Eastern Italy (Fig. 1), closed at 'Vo Destro' gauging station (drainage area c.12000 km^2). The Adige River is the second longest Italian river, with the typical natural streamflow regime of the Alpine region showing two seasonal maxima, one occurring in spring-summer due to snow and glacier melt, and the other in autumn triggered by cyclonic storms (Chiogna et al., 2016; Mallucci et al., 2019). Recent analysis of historical hydro-climatic trends revealed that the basin is sensitive to climate change with ongoing reduction of winter snowfall and anticipation of

194   snow-melting season (Diamantini et al., 2018; Lutz et al., 2016; Mallucci et al., 2019),

195   which are likely to alter its flow regime by the second half of 21st century (Majone et al.,

196   2016). Such modifications may have relevant consequences for hydropower production,

197   which is particularly relevant in the watershed (Bellin et al., 2016; Zolezzi et al., 2009).

198

199

200   *2.2 Observational datasets*

201   *2.2.1 Flow data*

202   The regional precipitation and temperature dataset ADIGE (Mallucci et al., 2019) was used

203   as meteorological forcing for hydrologic modelling. This dataset provides daily precipitations

204   and temperatures between 1956 and 2013 at the spatial resolution of 1 km. It has been

205   developed by interpolating the measurements available at the meteorological stations within

206   and nearby the river basin by means of kriging with external drift (Goovaerts, 1997; Mallucci

207   et al., 2019). To comply with the computational grid adopted in the hydrologic modeling, the

208   ADIGE dataset was aggregated to 5-km.

209   Daily streamflow data collected at 14 gauging stations (Fig.S1 in SM) were provided by the

210   Hydrological Office of the Autonomous Provinces of Trento (www.floods.it) and Bolzano

211   (www.provincia.bz.it/hydro). Stations were selected according to the following criteria: i)

212   observational period including the 1989–2013 time-frame used for calibration and validation

213   of the hydrologic model; ii) limited gaps in records; iii) large distance from upstream

214   reservoirs if present; and, iv) broad spatial coverage including the major tributaries of the

215   Adige River. The gauging stations were distributed in sub-catchments of different size,

216   elevation, geology and land-cover and were therefore representative of the hydrologic

217   regimes of the Adige basin.

218

219   *2.2.2 Macroinvertebrate data*

220   Macroinvertebrate data were collected by the Environmental Protection Agencies of the

221   Provinces of Trento and Bolzano as part of their institutional monitoring programmes (Larsen

222   et al., 2019). Sampling was performed according to the multi-habitat sampling approach

223   defined in the AQEM (http://www.aqem.de/) protocol: 10-replicate Surber samples were

224   collected within a 20-50 m reach in proportion to the micro-habitats present (Hering et al.,

225   2004). We selected 100 locations (Fig.1) for which streamflow regime was almost pristine

226 (i.e. no major in-stream structure or impoundments upstream), mostly within 1st and 2nd order
227 reaches, with elevation ranging from 170 to 1900 m a.s.l. Samples were collected in the
228 period 2009-2015, and sites were visited several times per year (median = 3), primarily in
229 spring and autumn. Macroinvertebrate densities were averaged over all samples to remove
230 seasonal effects, thereby obtaining the typical community composition of each site.

231 *2.2.3 Reach-scale environmental data*
232 Two additional reach-scale environmental variables were included in the analyses besides
233 streamflow regime: the proportion of agricultural land-use ("Agr.landuse"), calculated within
234 1-km buffer around each sampling location, and the water physico-chemical quality, as
235 expressed by the "LIMeco" index (Livello di Inquinamento da Macrodescrittori per lo stato
236 ecologico), one of the official WFD water quality indicators used to assess the ecological
237 status of water courses in Italy (European Commission, 2000). This is a multi-metric
238 indicator assigning quality scores based on threshold levels for concentration of oxygen,
239 ammonia, nitrate and total phosphorus in waters (see Azzellino et al., 2015). These
240 environmental descriptors were included as covariates in the quantification of flow-ecology
241 relationship because of their known influence on the composition of benthic invertebrates in
242 the area (Larsen et al., 2019).
243
244

245 **2.3 Hydrologic simulations**
246 Hydrologic simulations were performed at the daily time scale with the HYPERstreamHS
247 model (Avesani et al., 2020; Laiti et al., 2018), which couples the HYPERstream routing
248 scheme (recently proposed by Piccolroaz et al., 2016) with a continuous SCS-CN module for
249 surface and subsurface flow generation (Michel et al., 2005). HYPERstream routing scheme
250 is specifically designed to couple with climate models and, in general, with gridded
251 meteorological datasets. HYPERstream inherits the computational grid of the climatic model,
252 or of the gridded product providing the meteorological forcing, and preserves
253 geomorphological dispersion due to the structure of the river network (Rinaldo et al., 1991),
254 regardless of grid resolution. In previous studies, the SCS-CN runoff module was
255 successfully applied to two tributaries of the Adige River (Bellin et al., 2016; Piccolroaz et
256 al., 2015) and in this study it is coupled with a non-linear bucket model for soil dynamics
257 (Majone et al., 2010). For a detailed description of the hydrologic modeling framework see
258 Laiti et al., (2018) and Avesani et al. (2020).

259   The hydrologic model was calibrated against daily streamflow observations in the time
260   window 1989-2013 using the ADIGE dataset. The parameters space was explored for
261   optimality, according to the Nash-Sutcliffe efficiency index (NSE; Nash & Sutcliffe, 1970),
262   by using the Particle Swarming Optimization algorithm (Kennedy & Eberhart, 1995). NSE
263   was selected because of its effectiveness in assessing the performance of hydrologic models
264   in reproducing observed streamflows. NSE can be considered satisfactory when larger than
265   0.5 (Moriasi et al., 2007). Because hydrologic modeling was tailored to reproduce streamflow
266   at unimpacted locations, four headwater gauging stations (Vermiglio, Rio Funes, Aurino and
267   Gadera, see Fig. S1 in SM) were used in a multisite calibration framework (i.e. NSE was
268   defined as the average of individual efficiencies from the four selected stations), whereas
269   other five headwater stations distributed across the basin (Saltusio, Vipiteno, Anterselva,
270   Trento and Bronzolo, Fig. S1 in the SM) were used for validation. The first two years of the
271   time series, 1989 and 1990, were used as spin-up for the simulations and therefore were
272   excluded from the computation of NSE. Finally, we used the calibrated hydrologic model to
273   simulate streamflow time series (1991-2013) at the 100 gauged and ungauged locations
274   where biological data were available (see Sect. 2.2.2 and Fig. 1).

275

276   *2.4 Hydrologic classification*
277   Simulated streamflow time series at the 100 locations were first normalised by their mean
278   annual discharge (MAD) to allow comparison across streams (e.g Rosenfeld, 2017). From an
279   ecological perspective, this measure is preferable than the absolute discharge (e.g. Tennant,
280   1976). Then, we classified streamflow regimes according to their typical seasonality as
281   follows. First, we calculated the mean monthly hydrographs for each location from the MAD-
282   normalised daily streamflow time series (Fig. S2 in SM); then we performed a Principal
283   Component Analysis (PCA) on the resulting hydrographs to synthesise similarities among
284   locations using the first two PC axes. Location scores on the two axes were then weighted by
285   the proportion of variance explained in the PCs and used as synthetic variables in order to
286   cluster the locations based on their flow regime (see e.g. Belmar et al., 2011). A flexible-beta
287   hierarchical clustering approach was used, with recommended value of beta= - 0.25 (Belmar
288   et al., 2011; Legendre & Legendre, 2012; Mazor et al., 2018) that provides an intermediate
289   solution between chaining obtained via single linkage and space dilation deriving from
290   complete linkage. Three distinct flow regime classes were then identified (see Results). To
291   further validate the degree of separation among the three classified regimes, we run a

9

292   Permutational Multivariate Analysis of Variance (PERMANOVA; Anderson, 2017) based on

293   the Euclidean distance matrix of the weighted PCA scores.

294

295

296   *2.5 Hydrologic metrics*

297   We used the 23 years MAD-normalised daily streamflow values to calculate 34 hydrologic

298   metrics following the Indicator of Hydrologic Alteration (IHA; Richter et al., 1997) approach

299   (Tab.1), implemented in R software with the "IHA" package (R Core Team, 2019). These

300   metrics quantify ecologically-relevant aspects of the flow regimes related to magnitude,

301   duration, frequency, timing and rate of change. As an exploratory step, and to visualise and

302   further validate the separation of the hydrologic classes in the multidimensional space defined

303   by the hydrologic metrics, we plotted the streams on the first two PCA axes derived from the

304   correlation matrix of the IHA metrics. However, our main interest was to quantify flow-

305   ecology relationships within the distinct hydrologic regimes considered as management units.

306   To this end, and to derive easily interpretable synthetic axes, we run a PCA separately within

307   each classified flow regime. This also reduced the collinearity of the multiple IHA metrics

308   (Olden & Poff, 2003). The first two PC axes were subsequently used as predictors in stream-

309   network models for quantifying flow-ecology relationships. In particular, we referred to the

310   loading of the IHA metrics on the PC axes for interpreting the hydrologic characterisation of

311   the flow-ecology relationships (Tab. 2).

312

313

314   *2.6 Data analysis*

315   We derived a set of taxonomic and functional metrics from the macroinvertebrate community

316   data. These included: taxonomic richness, Shannon diversity (as effective number of species

317   of order q=1; Jost, 2006), Functional Dispersion (FDis, which is minimally influenced by

318   taxonomic richness), the proportion of different feeding groups (i.e. grazers, shredders,

319   gatherers, filterers and predators), the proportion of relatively small and large sized (range

320   0.25-0.5 mm and 20-40 mm, respectively) invertebrates, and the WFD Star_ICMi index. The

321   Star_ICMi is the official Biological Quality Element used in Italy to classify the status of

322   running water in line with the WFD requirements (Buffagni et al., 2006; Buffagni & Erba,

323   2007). The index is formulated combining six normalised and weighted metrics, including

324   richness, diversity and taxa sensitivity to organic pollution (Buffagni et al., 2006).

325   Information for functional traits of the taxa was gathered from the online database of

326   freshwater ecology (www.freshwaterecology.info; Schmidt-Kloiber & Hering, 2015). For the

327   calculation of FDis, we included 13 traits (Tab. S1) in order to provide an inclusive measure

328   of functional diversity. For the examination of flow-ecology relationships, we specifically

329   focused on feeding traits as they convey information about the functional role of organisms in

330   the ecosystems, and size traits that are a proxy of multiple life-history characteristics like e.g.

331   life cycle duration, longevity (Poff et al., 2006). Feeding information was available for all

332   taxa included in the analysis, whereas size traits were available for about 50% of the taxa.

333

334   *2.6.1 Spatial stream-network models*

335   Spatial stream-network models (SSN; Ver Hoef et al., 2014; Ver Hoef & Peterson, 2010)

336   were run separately for each flow regime to quantify the relation between the biotic metrics

337   and the hydrologic predictors (i.e., PC axes derived from the IHA metrics), while accounting

338   for the autocorrelation structures of dendritic networks. The LIMeco index and Agr.landuse

339   indicator were included as additional covariates in the models. ArcMap 10.5 and the STARS

340   toolset (Peterson & Hoef, 2014) were used to generate the spatial data necessary to analyse

341   stream-network models. The full set of autocovariance functions were used to model spatial

342   autocorrelation, including Euclidean, in-stream flow-connected (locations in which water

343   flows from one to the other) and flow-unconnected (connected within the network, but not

344   reflecting the directionality of the water flow) functions. This approach allows accounting

345   simultaneously for the along-channel and across-basin (flow-unconnected and Euclidean,

346   respectively) patterns of autocorrelation, while also distinguishing locations linked by direct

347   water flow (i.e. flow-connected). In particular, SSN models take the form:

348

349    $y = X\beta + z_{TU} + z_{TD} + z_E + \varepsilon$ (1)

350

351   where y is the response variable (i.e., macroinvertebrate metrics in this study), X is the matrix

352   of predictors (hydrologic PCs, LIMeco, and Agr.landuse) with associated β regression

353   parameters, while $z_{TU} + z_{TD} + z_E$ are zero-mean random variables with autocorrelation

354   structure based on tail-up (TU), tail-down (TD) and Euclidean (E) functions, respectively,

355   and ε is the random independent error. The TU and TD functions are moving-averages

356   functions autocorrelated in one direction: upstream the former and downstream the latter.

357   Tail-up function assigns different weights to locations upstream of a given site according to

358   the catchment area used here as a proxy of discharge. In this way, the moving-average

359   autocorrelation gets split at confluences so that upstream locations with larger catchments

360   have a stronger influence on downstream communities. The reader can refer to Peterson et al.

361   (2013) and Ver Hoef et al. (2010) for a detailed description of the SSN framework.

362

363   Biotic metrics expressed as proportions (feeding and size traits) were logit-transformed as

364   recommended (Warton & Hui, 2011), and maximum-likelihood was used for parameter

365   estimation in all SSN models. For each biotic metric, the most supported model was selected

366   based on the root mean-square prediction error (RMSPE). The model was developed in a

367   stepwise fashion, following guidelines provided in Ver Hoef et al. (2014). We first included

368   all predictors (hydrologic PCs, LIMeco, Agr.landuse), and the full set of autocovariance

369   functions (i.e. tail-up, tail-down and Euclidean). Then we manually removed the non-

370   significant predictors and selected the final model with the lowest RMSPE. Our main interest

371   was to identify the most important predictors while accounting for the overall spatial

372   autocorrelation. Therefore, we did not specifically refine the shape of the autocorrelation

373   functions and used the default exponential form in each model (Garreta et al., 2009; Isaak et

374   al., 2014). The SSN package (Ver Hoef et al. 2014) for R software (R Core Team, 2019) was

375   used to run the stream-network models.

376   Row data will be archived in repository upon acceptance of the manuscript.

377

378

379   ## 3. Results

380

381   *3.1 Hydrologic simulations and classification*

382   The capability of HYPERstreamHS hydrologic model to reproduce the observed streamflow

383   time series in the Adige River was evaluated for the period 1991- 2013 by computing NSE at

384   the 9 gauging stations described in Sect. 2.4 (see also Fig. S1 in SM). The parameters of the

385   hydrologic model were inferred by maximizing the average NSE at Vermiglio, Rio Funes,

386   Aurino and Gadera gauging stations. Calibration produced a satisfactory mean NSE of 0.623

387   (range: 0.58-0.70; Fig. S3). At the validation stations, mean NSE was 0.620 (range: 0.48-

388   0.79), with lower values in the smaller subcatchments (Saltusio, Isarco, Anterselva; Fig. S3),

389   and higher values at the larger downstream subcatchments of Trento and Bronzolo (0.74 and

390   0.79, respectively; Fig. S3 in SM). Remarkably, NSE did not deteriorate in validation,

391   suggesting that model parameters are representative of the entire river basin.

393 The calibrated model was used to simulate flow time series for the period 1991-2013 in the

394 100 reference locations for which biological data were available, and to perform the

395 hydrologic classification. Three hydrologic classes with distinct flow regimes were identified

396 by the flexible beta-clustering of the first two weighted PC scores (explaining 92% of the

397 variation) derived from the scaled monthly hydrographs (Fig. 2). The first hierarchical

398 division separated typical "pluvial" streams (n=38), with peak flow in autumn, from those

399 with spring and summer peaks. The second division further distinguished streams with

400 "nivo-glacial" regime (n=30) with summer peak flows and winter low flows, from

401 intermediate "nivo-pluvial" streams (n=32), with earlier spring peak flows and relatively

402 higher autumn flows. These flow regimes largely correspond to the definition of Krenal,

403 Kryal and Rhithral streams, respectively, suggested by Brown et al. (2003). A

404 PERMANOVA based on Euclidean distances further validated the significant separation

405 among the three groups with $R^2 = 0.85$.

406 Fig. 1 shows the distribution of the flow regime classes in the Adige River network. The three

407 flow regimes were distributed along an altitudinal gradient, which reflects also the gradient of

408 anthropogenic influence in the catchment (Fig. 3). Indeed, pluvial streams at lower altitude

409 were characterised by more eutrophic (higher LIMeco scores) waters and higher proportion

410 of agricultural land-use in the adjacent area. The separation of the three flow regimes over

411 these environmental descriptors further supported the classification derived from the

412 streamflow series.

414 The three hydrologic classes identified in the previous step formed three groups in the first

415 PCA factorial plane (i.e., the first two PCs) derived from IHA metrics, explaining about 80%

416 of the total variation (Fig. 4). This analysis provided additional evidence of the separation

417 among the flow regimes, and allowed identifying the metrics that differed the most among

418 them. For instance, as also evident from the annual hydrographs shown in Fig. 2, nivo-glacial

419 streams displayed higher flow maxima during summer months (June, July; Fig. 4 and 5) as

420 well as faster fall and rise rates. Conversely, streams with pluvial regime showed higher flow

421 minima (e.g. 30 Day Min) and Base index, but more frequent low flow events (Fig. 5). Nivo-

422 pluvial streams systematically showed flow metrics that were intermediate between the nivo-

423 glacial and pluvial regimes.

424 The first two PCA axes extracted separately within each flow regime, accounted for 75%,

425 81% and 76% of variation in IHA metrics across the nivo-glacial, nivo-pluvial and pluvial

426   regime, respectively. The loadings of the IHA metrics on the PC axes are shown in Tab. 2,

427   and were used for the interpretation of flow-ecology relationships examined in the ensuing

428   section. The first PCA axis was strongly associated with measures of extreme flow conditions

429   (e.g. 90 Day Max) consistently across the three hydrologic classes. Loadings of the other IHA

430   metrics on the PC axes were more variable across flow regimes (Tab. 2).

431

432

433   *3.2 Flow-ecology relationship*

434   A total of 64 invertebrate taxa were identified, mostly at family and genus level (see Tab.

435   S2). Flow-ecology models identified several significant relations with the hydrologic metrics,

436   as synthesised by the PC axes, and the covariates related to water quality and land-use (see

437   Tab. 3). The relations differed among the flow regimes both in terms of explained variance

438   and selected covariates. In the nivo-glacial streams, SSN models included the first hydrologic

439   PC in six out of the eleven biotic metrics analysed, although the contribution of the

440   hydrologic PC was significant only in explaining the variation in proportion of grazers and

441   size traits (i.e. small and large body size). In the nivo-pluvial streams, hydrologic PCs were

442   also included in six biotic metrics analysed, but were only significant in explaining the

443   variation in size traits. In pluvial streams, conversely, hydrologic PCs were significant

444   predictors for four biotic metrics, including richness, FDis, and the proportion of grazers and

445   filterers. Overall, the influence of water quality (LIMeco index) and agricultural land-use on

446   macroinvertebrate communities was evident, especially for pluvial streams at lower altitude,

447   in which these parameters were significant for five out of eleven biotic metrics.

448   Few response variables responded consistently to the hydrologic metrics across the different

449   flow regimes, and rather, flow-ecology relationships often displayed opposite patterns

450   (opposite sign of hydrologic PCs in Tab. 3). For instance, in nivo-glacial and pluvial streams,

451   taxonomic richness and grazers proportion responded differently to maximum flow and

452   annual flow CV (Fig. 6). Nivo-pluvial and pluvial streams also displayed some opposite

453   patterns such as the relation of FDis with mean June discharge (Fig. 6). Other biotic metrics,

454   such as Shannon diversity, the Star_ICMi index and the proportion of shredders and predators

455   responded almost exclusively to water quality or land-use (Tab. 3), implying a low sensitivity

456   to flow characteristics. Size traits appeared sensitive to flow characteristics in both nivo-

457   glacial and nivo-pluvial streams, whereas they were primarily influenced by land-use in

458   pluvial streams.

459   Overall, spatial autocorrelation, considering the Euclidean, flow-connected and flow-
460   unconnected dimension (i.e. z_{TU}, z_{TD}, z_E in equation 1), explained a larger proportion of
461   variance (more than 50% on average) than the model predictors ($X\beta$ in equation 1) which
462   explained 15-22% of the variance. Spatial effects accounted for 90% of the variance for
463   some biotic metrics (e.g. proportion of gatherers, filterers, Star_ICMi). Autocorrelation was
464   particularly important for nivo-pluvial streams (mean across biotic metrics: 0.8), and
465   relatively weaker in pluvial flow-regime (mean: 0.55), where we observed the only case
466   where model covariates explained most of the variance (shredders *vs* LIMeco).
467
468

469   ## 4. Discussion

470
471   The HYPERSstreamHS hydrologic model was calibrated and applied within the Adige River
472   basin to obtain a reliable representation of streamflow at the 100 biological sampling stations.
473   Validation with gauging stations not used in calibration showed that HYPERSstreamHS
474   successfully reproduced streamflow timing, and thus allowed deriving streamflow
475   characteristics at the ungauged locations.
476   An additional validation of the hydrologic model stems from the consistent patterns of flow-
477   ecology relationships obtained from the observed and simulated streamflow. For instance,
478   Fig. S4 shows how the relationship between taxon richness and IHA metrics was conserved
479   across observed and simulated flow data, in the locations where measured streamflow time
480   series were available. This is important when hydrologic models are used to investigate
481   ecological responses (Kiesel et al., 2020). Indeed, the uncertainty associated with modelled
482   streamflow is acknowledged as one of the most important limiting factors hampering the
483   study of flow-ecology relationship at the pan-European scale (Vigiak et al., 2018).
484   We identified three flow regimes representing typical hydrologic patterns of the Alpine
485   region. Low-order streams at higher elevation are fed primarily by glacial melt, snowmelt and
486   associated groundwater flow; streams at intermediate elevations by snowmelt and rain, and
487   those at lower elevation mirroring rainfall timing. The three flow regimes also were well-
488   separated along a gradient of anthropogenic influence represented by water quality and
489   riparian land-use. This further highlights how classifying regimes can help minimising the
490   effect of confounding factors in flow-ecology research (Bruckerhoff et al., 2019).

491   While realistically representing a gradient of conditions, the three regimes were distinct

492   enough to form separate groups according to both mean annual flow series and IHA metrics.

493   As such, they showed distinct flow-ecology relationships, especially with measures of

494   maximum and minimum discharge and its temporal variation (i.e. those metrics with the

495   strongest loadings on the hydrologic PCs used in stream-network models; Tab. 2 and Fig. 6).

496

497   Few studies have compared flow-ecology relations across classified flow regimes (e.g.

498   Bruckerhoff et al., 2019; Mims & Olden, 2012), showing that ecological responses can often

499   diverge. Had we combined all streams in the same analysis, we would have drawn different

500   conclusions regarding the response of some biotic metrics (e.g., taxon richness, grazers; *cfr*

501   grey dashed line with individual fits in Fig. 6). This has both practical and fundamental

502   implications. From an applied perspective, it implies that ecological responses to flow

503   alterations can be contingent on local eco-hydrologic conditions, a caveat which must be

504   considered when setting regional flow standards. On a more fundamental level, it indicates

505   that the often observed nonlinear flow-ecology relationships (Rosenfeld, 2017) can reflect the

506   distinct response of multiple flow regimes in the basin. More generally, the "shape" of flow-

507   ecology relationships is likely to be scale-dependent and determined by the range of

508   hydrologic conditions in the region and the size of the species pool included.

509

510   SSN models revealed how the STAR_ICMi index was significantly influenced by streams

511   physico-chemical parameters and riparian land-use. In agreement with recent investigations

512   (Larsen et al., 2019; Quadroni et al., 2017), these results provide additional evidence of the

513   limited sensitivity of WFD biological quality indicators, such the Star_ICMi index, to stream

514   hydrologic conditions. Nonetheless, Fig.6 shows that the minimum scores of the index

515   declined with increasing magnitude of minimum discharge, consistently across flow regimes.

516   In other words, this type of response indicates that flow conditions may represent a limiting

517   factor that locally lowers the minimum score of the Star_ICMi index. Quantile regression

518   approaches have been used in flow-ecology research to examine these type of responses

519   because flow conditions are more likely to affect the upper or lower distribution of biotic

520   metrics, rather than the mean (Fornaroli et al., 2015; Konrad et al., 2008; Larsen et al., 2019;

521   Mims & Olden, 2012). However, as most present bioindicators (Friberg, 2014), the

522   Star_ICMi is designed to reflect organic pollution and habitat degradation, and should be

523   used for hydrologic assessment or guide *e-flows* with great caution. Further effort is needed

524 to identify flow-sensitive indicators to be included in assessment schemes like the one of the
525 European WFD.

526 Species life-history traits could provide a mechanistic link between river biota and flow
527 conditions that could be valid across large spatial scales (Heino et al., 2013; Mims & Olden,
528 2012). In the Adige River basin, the proportion of invertebrate grazers and body size structure
529 appeared relatively sensitive to hydrologic conditions across flow regimes and thus deserve
530 further investigation. The sensitivity of grazers to flow conditions can derive from their
531 reliance on attached algae as observed in other studies (Buchanan et al., 2013; Doretto et al.,
532 2020; Kennen et al., 2010). The relative decline of small taxa with the magnitude of flow
533 peaks (and the concomitant increase of larger taxa; Tab. 3) may reflect their sensitivity to
534 shear stress (e.g. Merigoux & Doledec, 2004). However, detailed information on body size
535 was not available for many taxa, and this response requires further examination.

536

537 The three identified flow regimes formed geographically separated clusters along a north-
538 south axis, reflecting the orography of the basin. While this further validates our flow regime
539 classification, it also introduces possible autocorrelation issues. SSN models revealed that
540 most variation in macroinvertebrate metrics was in fact associated with spatial patterns. This
541 is typical for communities inhabiting complex habitats, such as river networks, whose
542 geometry and flow directionality influence environmental and ecological dynamics (Frieden
543 et al., 2014; Isaak et al., 2014; Larsen et al., 2019). However, spatial effects might be
544 particularly relevant for flow-ecology studies when these are paralleled with flow regime
545 classification in which sites might be locally clumped (e.g. Bruckerhoff et al., 2019; Snelder
546 & Booker, 2013). Ignoring such spatial dependency could lead to increased Type I error rates
547 ("false positive"; Legendre & Legendre, 2012), with important implications for the success of
548 *e-flows* design.

549

550 An additional issue to consider is that, although we selected streams with no evident
551 alteration of flow regime, the influence of other disturbance on stream invertebrates was
552 evident. For instance, Shannon diversity and the proportion of shredders and predators
553 declined with increasing agricultural land-use and degraded water quality, and did so
554 consistently across flow regimes. This is not surprising and in line with a recent study that
555 included a larger sample of locations throughout the basin (Larsen et al., 2019). However,
556 this highlights how defining a baseline flow-ecology relationship under natural conditions
557 might become increasingly difficult as river catchments are modified globally (Tickner et al.,

558   2020). In addition, alteration of flow regimes is often accompanied by changes in water

559   temperature and in-stream habitat structure (e.g. Zolezzi et al., 2011). Therefore, non-

560   hydrologic factors must be incorporated in *e-flow* frameworks to identify circumstances that

561   might limit the desired outcome of flow management (Poff, 2018).

562

563   At the management level of *e-flows* setting, the present work represents the first classification

564   of natural flow regimes in Italy that is paralleled by an ecological assessment. Previous

565   catchment regionalisation schemes were produced at the national scale (Di Prinzio et al.,

566   2011), but they focused primarily on estimating streamflow at ungauged sites. Results

567   demonstrated that flow-ecology relationships can substantially vary among flow regimes,

568   highlighting the importance of developing *e-flows* tailored to specific eco-hydrologic

569   contexts. Moreover, although analyses were conducted within a single river basin, and thus

570   minimised the influence of larger-scale confounding factors, spatial patterns accounted for

571   most of the variance in the data. The importance of using spatially-explicit approaches to

572   model empirical data in river networks is increasingly recognised (Frieden et al., 2014; Isaak

573   et al., 2017; Larsen et al., 2019), and our results further support their application in flow-

574   ecology research (Bruckerhoff et al., 2019).

575   In conclusion, we addressed three main challenges of flow-ecology research derived from:

576   i) the limited availability of flow series, ii) the natural variability of flow regimes and iii) the

577   spatial autocorrelation unique to dendritic river networks. In doing so we also completed the

578   first two steps of the ELOHA framework (Poff et al., 2010) that, to our knowledge, was

579   applied for the first time in a very heterogeneous Alpine river catchment.

580   Future developments should address the challenge of incorporating hydrologic variability

581   when setting environmental flows, and of assessing the ecological effects of specific flow

582   events or sequence of events without relying on stationary long-term flow records as baseline

583   reference (Horne et al., 2019; Poff, 2018). The framework presented in this paper can could

584   thus be extended to include future climate scenarios to feed the hydrologic model. Simulated

585   projections of streamflow could then be used to estimate future ecological responses to flow

586   alteration.

587

588

589

590

Acknowledgements

References

Anderson, M. J. (2017). Permutational Multivariate Analysis of Variance (PERMANOVA). In *Wiley StatsRef: Statistics Reference Online* (pp. 1–15). American Cancer Society. https://doi.org/10.1002/9781118445112.stat07841

Arthington, A. H., Bhaduri, A., Bunn, S. E., Jackson, S. E., Tharme, R. E., Tickner, D., et al. (2018). The Brisbane Declaration and Global Action Agenda on Environmental Flows (2018). *Frontiers in Environmental Science*, *6*. https://doi.org/10.3389/fenvs.2018.00045

Avesani, D., Galletti, A., Piccolroaz, S., Bellin, A., & Majone, B. (2020). A dual layer MPI continuous large-scale hydrological model including Human Systems.

Azzellino, A., Canobbio, S., Çervigen, S., Marchesi, V., & Piana, A. (2015). Disentangling the multiple stressors acting on stream ecosystems to support restoration priorities. *Water Science & Technology*, *72*(2), 293. https://doi.org/10.2166/wst.2015.177

Bellin, A., Majone, B., Cainelli, O., Alberici, D., & Villa, F. (2016). A continuous coupled hydrological and water resources management model. *Environmental Modelling & Software*, *75*, 176–192. https://doi.org/10.1016/j.envsoft.2015.10.013

Belmar, Velasco, J., & Martinez-Capel, F. (2011). Hydrological Classification of Natural Flow Regimes to Support Environmental Flow Assessments in Intensively Regulated

624   Mediterranean Rivers, Segura River Basin (Spain). *Environmental Management*,

625   *47*(5), 992. https://doi.org/10.1007/s00267-011-9661-0

626 Beven, K. (2012). *Rainfall-Runoff Modelling: The Primer*. Wiley-Blackwell.

627 Booker, D. J., Snelder, T. H., Greenwood, M. J., & Crow, S. K. (2015). Relationships

628   between invertebrate communities and both hydrological regime and other

629   environmental factors across New Zealand's rivers. *Ecohydrology*, *8*(1), 13–32.

630   https://doi.org/10.1002/eco.1481

631 Brown, L. E., Hannah, D. M., & Milner, A. M. (2003). Alpine Stream Habitat Classification:

632   An Alternative Approach Incorporating the Role of Dynamic Water Source

633   Contributions. *Arctic, Antarctic, and Alpine Research*, *35*(3), 313–322.

634   https://doi.org/10.1657/1523-0430(2003)035[0313:ASHCAA]2.0.CO;2

635 Bruckerhoff, L. A., Leasure, D. R., & Magoulick, D. D. (2019). Flow–ecology relationships

636   are spatially structured and differ among flow regimes. *Journal of Applied Ecology*,

637   *56*(2), 398–412. https://doi.org/10.1111/1365-2664.13297

638 Buchanan, C., Moltz, H. L. N., Haywood, H. C., Palmer, J. B., & Griggs, A. N. (2013). A test

639   of The Ecological Limits of Hydrologic Alteration (ELOHA) method for determining

640   environmental flows in the Potomac River basin, U.S.A. *Freshwater Biology*, *58*(12),

641   2632–2647. https://doi.org/10.1111/fwb.12240

642 Carrara, F., Altermatt, F., Rodriguez-Iturbe, I., & Rinaldo, A. (2012). Dendritic connectivity

643   controls biodiversity patterns in experimental metacommunities. *Proceedings of the*

644   *National Academy of Sciences*, *109*(15), 5761–5766.

645   https://doi.org/10.1073/pnas.1119651109

646 Chiogna, G., Majone, B., Cano Paoli, K., Diamantini, E., Stella, E., Mallucci, S., et al.

647   (2016). A review of hydrological and chemical stressors in the Adige catchment and

648   its ecological status. *Science of The Total Environment*, *540*, 429–443.

649   https://doi.org/10.1016/j.scitotenv.2015.06.149

650 Couto, T. B., & Olden, J. D. (2018). Global proliferation of small hydropower plants –

651   science and policy. *Frontiers in Ecology and the Environment*, *16*(2), 91–100.

652   https://doi.org/10.1002/fee.1746

653 De Pauw, N., Gabriels, W., & Goethals, P. L. M. (2006). River Monitoring and Assessment

654   Methods Based on Macroinvertebrates. In *Biological Monitoring of Rivers* (pp. 111–

655   134). Wiley-Blackwell. https://doi.org/10.1002/0470863781.ch7

656 Di Prinzio, M., Castellarin, A., & Toth, E. (2011). Data-driven catchment classification:

657   application to the pub problem. *Hydrology and Earth System Sciences*, *15*(6), 1921–

658   1935. https://doi.org/10.5194/hess-15-1921-2011

659 Diamantini, E., Lutz, S. R., Mallucci, S., Majone, B., Merz, R., & Bellin, A. (2018). Driver

660   detection of water quality trends in three large European river basins. *Science of The*

661   *Total Environment*, *612*, 49–62. https://doi.org/10.1016/j.scitotenv.2017.08.172

662 Doretto, A., Bona, F., Falasco, E., Morandini, D., Piano, E., & Fenoglio, S. (2020). Stay with

663   the flow: How macroinvertebrate communities recover during the rewetting phase in

664   Alpine streams affected by an exceptional drought. *River Research and Applications*,

665   *36*(1), 91–101. https://doi.org/10.1002/rra.3563

666 European Commission. (2000). Directive 2000/60/EC of 20 December 2000 of the European

667   Union and of the Council establishing a framework for community action in the field

668   of water policy. Official Journal of the European Communities.

669 Fornaroli, R., Cabrini, R., Sartori, L., Marazzi, F., Vracevic, D., Mezzanotte, V., et al. (2015).

670   Predicting the constraint effect of environmental characteristics on macroinvertebrate

671   density and diversity using quantile regression mixed model. *Hydrobiologia*, *742*(1),

672   153–167. https://doi.org/10.1007/s10750-014-1974-6

673 Friberg, N. (2014). Impacts and indicators of change in lotic ecosystems. *Wiley*

674   *Interdisciplinary Reviews: Water*, *1*(6), 513–531. https://doi.org/10.1002/wat2.1040

675 Frieden, J. C., Peterson, E. E., Angus Webb, J., & Negus, P. M. (2014). Improving the

676   predictive power of spatial statistical models of stream macroinvertebrates using

677   weighted autocovariance functions. *Environmental Modelling & Software*, *60*, 320–

678   330. https://doi.org/10.1016/j.envsoft.2014.06.019

679 Garreta, V., Monestiez, P., & Ver Hoef, J. M. (2009). Spatial modelling and prediction on

680   river networks: up model, down model or hybrid? *Environmetrics*, n/a-n/a.

681   https://doi.org/10.1002/env.995

682 Goovaerts, P. (1997). *Geostatistics for Natural Resources Evaluation*. Oxford University

683   Press.

684 Green, P. A., Vörösmarty, C. J., Harrison, I., Farrell, T., Sáenz, L., & Fekete, B. M. (2015).

685   Freshwater ecosystem services supporting humans: Pivoting from water crisis to

686   water solutions. *Global Environmental Change*, *34*, 108–118.

687   https://doi.org/10.1016/j.gloenvcha.2015.06.007

688 Grill, G., Lehner, B., Thieme, M., Geenen, B., Tickner, D., Antonelli, F., et al. (2019).

689   Mapping the world's free-flowing rivers. *Nature*, *569*(7755), 215–221.

690   https://doi.org/10.1038/s41586-019-1111-9

691 Heino, J., Schmera, D., & Erős, T. (2013). A macroecological perspective of trait patterns in

692   stream communities. *Freshwater Biology*, *58*(8), 1539–1555.

693   https://doi.org/10.1111/fwb.12164

694 Horne, A. C., Nathan, R., Poff, N. L., Bond, N. R., Webb, J. A., Wang, J., & John, A. (2019).

695   Modeling Flow-Ecology Responses in the Anthropocene: Challenges for Sustainable

696   Riverine Management. *BioScience*, *69*(10), 789–799.

697   https://doi.org/10.1093/biosci/biz087

698 Isaak, D. J., Peterson, E. E., Ver Hoef, J. M., Wenger, S. J., Falke, J. A., Torgersen, C. E., et

699   al. (2014). Applications of spatial statistical network models to stream data: Spatial

700   statistical network models for stream data. *Wiley Interdisciplinary Reviews: Water*,

701   *1*(3), 277–294. https://doi.org/10.1002/wat2.1023

702 Isaak, D. J., Ver Hoef, J. M., Peterson, E. E., Horan, D. L., & Nagel, D. E. (2017). Scalable

703   population estimates using spatial-stream-network (SSN) models, fish density

704   surveys, and national geospatial database frameworks for streams. *Canadian Journal*

705   *of Fisheries and Aquatic Sciences*, *74*(2), 147–156. https://doi.org/10.1139/cjfas-

706   2016-0247

707 Jost, L. (2006). Entropy and diversity. *Oikos*, *113*(2), 363–375.

708   https://doi.org/10.1111/j.2006.0030-1299.14714.x

709 Kennedy, J., & Eberhart, R. (1995). Particle swarm optimization. In *Proceedings of ICNN'95*.

710 Kennen, J. G., Riva-Murray, K., & Beaulieu, K. M. (2010). Determining hydrologic factors

711   that influence stream macroinvertebrate assemblages in the northeastern US.

712   *Ecohydrology*, *3*(1), 88–106. https://doi.org/10.1002/eco.99

713 Kiesel, J., Kakouei, K., Guse, B., Fohrer, N., & Jähnig, S. C. (2020). When is a hydrological

714   model sufficiently calibrated to depict flow preferences of riverine species?

715   *Ecohydrology*, *13*(3), e2193. https://doi.org/10.1002/eco.2193

716 Konrad, C. P., Brasher, A. M. D., & May, J. T. (2008). Assessing streamflow characteristics

717   as limiting factors on benthic invertebrate assemblages in streams across the western

718   United States. *Freshwater Biology*, *53*(10), 1983–1998.

719   https://doi.org/10.1111/j.1365-2427.2008.02024.x

720 Laiti, L., Mallucci, S., Piccolroaz, S., Bellin, A., Zardi, D., Fiori, A., et al. (2018). Testing the

721   Hydrological Coherence of High-Resolution Gridded Precipitation and Temperature

722   Data Sets. *Water Resources Research*, *54*(3), 1999–2016.

723   https://doi.org/10.1002/2017WR021633

724 Larsen, S., Bruno, M. C., Vaughan, I. P., & Zolezzi, G. (2019). Testing the River Continuum

725   Concept with geostatistical stream-network models. *Ecological Complexity*, *39*,

726   100773. https://doi.org/10.1016/j.ecocom.2019.100773

727 Larsen, S., Bruno, M. C., & Zolezzi, G. (2019). WFD ecological status indicator shows poor

728   correlation with flow parameters in a large Alpine catchment. *Ecological Indicators*,

729   *98*, 704–711. https://doi.org/10.1016/j.ecolind.2018.11.047

730 Legendre, P., & Legendre, L. (2012). *Numerical Ecology, Volume 24 - 3rd Edition*. Elsevier.

731   Retrieved from https://www.elsevier.com/books/numerical-ecology/legendre/978-0-

732   444-53868-0

733 Lutz, S. R., Mallucci, S., Diamantini, E., Majone, B., Bellin, A., & Merz, R. (2016).

734   Hydroclimatic and water quality trends across three Mediterranean river basins.

735   *Science of The Total Environment*, *571*, 1392–1406.

736   https://doi.org/10.1016/j.scitotenv.2016.07.102

737 Majone, B., Bertagnoli, A., & Bellin, A. (2010). A non-linear runoff generation model in

738   small Alpine catchments. *Journal of Hydrology*, *385*(1), 300–312.

739   https://doi.org/10.1016/j.jhydrol.2010.02.033

740 Majone, B., Villa, F., Deidda, R., & Bellin, A. (2016). Impact of climate change and water

741   use policies on hydropower potential in the south-eastern Alpine region. *Science of*

742   *The Total Environment*, *543*, 965–980. https://doi.org/10.1016/j.scitotenv.2015.05.009

743 Mallucci, S., Majone, B., & Bellin, A. (2019). Detection and attribution of hydrological

744   changes in a large Alpine river basin. *Journal of Hydrology*, *575*, 1214–1229.

745   https://doi.org/10.1016/j.jhydrol.2019.06.020

746 Mazor, R. D., May, J. T., Sengupta, A., McCune, K. S., Bledsoe, B. P., & Stein, E. D. (2018).

747   Tools for managing hydrologic alteration on a regional scale: Setting targets to protect

748   stream health. *Freshwater Biology*. https://doi.org/10.1111/fwb.13062

749 McGuire, K. J., Torgersen, C. E., Likens, G. E., Buso, D. C., Lowe, W. H., & Bailey, S. W.

750   (2014). Network analysis reveals multiscale controls on streamwater chemistry.

751   *Proceedings of the National Academy of Sciences*, *111*(19), 7030–7035.

752   https://doi.org/10.1073/pnas.1404820111

753 Merigoux, S., & Doledec, S. (2004). Hydraulic requirements of stream communities: a case

754   study on invertebrates. *Freshwater Biology*, *49*(5), 600–613.

755   https://doi.org/10.1111/j.1365-2427.2004.01214.x

756 Michel, C., Andréassian, V., & Perrin, C. (2005). Soil Conservation Service Curve Number

757   method: How to mend a wrong soil moisture accounting procedure? *Water Resources*

758   *Research*, *41*(2). https://doi.org/10.1029/2004WR003191

759 Mims, M. C., & Olden, J. D. (2012). Life history theory predicts fish assemblage response to

760   hydrologic regimes. *Ecology*, *93*(1), 35–45. https://doi.org/10.1890/11-0370.1

761 Navarro-Ortega, A., Acuña, V., Bellin, A., Burek, P., Cassiani, G., Choukr-Allah, R., et al.

762   (2015). Managing the effects of multiple stressors on aquatic ecosystems under water

763   scarcity. The GLOBAQUA project. *Science of The Total Environment*, *503–504*, 3–9.

764   https://doi.org/10.1016/j.scitotenv.2014.06.081

765 Olden, J. D., & Poff, N. L. (2003). Redundancy and the choice of hydrologic indices for

766   characterizing streamflow regimes. *River Research and Applications*, *19*(2), 101–121.

767   https://doi.org/10.1002/rra.700

768 Patrick, C. J., & Yuan, L. L. (2017a). Modeled hydrologic metrics show links between

769   hydrology and the functional composition of stream assemblages. *Ecological*

770   *Applications*, *27*(5), 1605–1617. https://doi.org/10.1002/eap.1554

771 Patrick, C. J., & Yuan, L. L. (2017b). Modeled hydrologic metrics show links between

772   hydrology and the functional composition of stream assemblages. *Ecological*

773   *Applications*, *27*(5), 1605–1617. https://doi.org/10.1002/eap.1554

774 Peterson, E. E., & Hoef, J. M. V. (2014). STARS: An ArcGIS Toolset Used to Calculate the

775   Spatial Information Needed to Fit Spatial Statistical Models to Stream Network Data.

776   *Journal of Statistical Software*, *56*(2). https://doi.org/10.18637/jss.v056.i02

777 Peterson, E. E., Ver Hoef, J. M., Isaak, D. J., Falke, J. A., Fortin, M.-J., Jordan, C. E., et al.

778   (2013). Modelling dendritic ecological networks in space: an integrated network

779   perspective. *Ecology Letters*, *16*(5), 707–719. https://doi.org/10.1111/ele.12084

780 Piccolroaz, S., Lazzaro, M. D., Zarlenga, A., Majone, B., Bellin, A., & Fiori, A. (2016).

781   HYPERstream: a multi-scale framework for streamflow routing in large-scale

782   hydrological model. *Hydrology and Earth System Sciences*, *20*(5), 2047–2061.

783   https://doi.org/10.5194/hess-20-2047-2016

784 Poff. (2018). Beyond the natural flow regime? Broadening the hydro-ecological foundation to

785   meet environmental flows challenges in a non-stationary world. *Freshwater Biology*,

786   *63*(8), 1011–1021. https://doi.org/10.1111/fwb.13038

787 Poff, Richter, B. D., Arthington, A. H., Bunn, S. E., Naiman, R. J., Kendy, E., et al. (2010).

788   The ecological limits of hydrologic alteration (ELOHA): a new framework for

789   developing regional environmental flow standards: Ecological limits of hydrologic

790   alteration. *Freshwater Biology*, *55*(1), 147–170. https://doi.org/10.1111/j.1365-

791   2427.2009.02204.x

792 Poff, N. L., Allan, J. D., Bain, M. B., Karr, J. R., Prestegaard, K. L., Richter, B. D., et al.

793   (1997). The Natural Flow Regime. *BioScience*, *47*(11), 769–784.

794 https://doi.org/10.2307/1313099

795 Poff, N. L., Olden, J. D., Vieira, N. K. M., Finn, D. S., Simmons, M. P., & Kondratieff, B. C.

796 (2006). Functional trait niches of North American lotic insects: traits-based ecological

797 applications in light of phylogenetic relationships. *Journal of the North American*

798 *Benthological Society*, *25*(4), 730–755. https://doi.org/10.1899/0887-

799 3593(2006)025[0730:FTNONA]2.0.CO;2

800 Quadroni, S., Crosa, G., Gentili, G., & Espa, P. (2017). Response of stream benthic

801 macroinvertebrates to current water management in Alpine catchments massively

802 developed for hydropower. *Science of The Total Environment*, *609*, 484–496.

803 https://doi.org/10.1016/j.scitotenv.2017.07.099

804 R Core Team. (2019). *R: A language and environment for statistical computing*. Vienna.

805 Richter, B., Baumgartner, J., Wigington, R., & Braun, D. (1997). How much water does a

806 river need? *Freshwater Biology*, *37*(1), 231–249. https://doi.org/10.1046/j.1365-

807 2427.1997.00153.x

808 Rinaldo, A., Marani, A., & Rigon, R. (1991). Geomorphological dispersion. *Water Resources*

809 *Research*, *27*(4), 513–525. https://doi.org/10.1029/90WR02501

810 Rosenfeld, J. S. (2017). Developing flow–ecology relationships: Implications of nonlinear

811 biological responses for water management. *Freshwater Biology*, *62*(8), 1305–1324.

812 https://doi.org/10.1111/fwb.12948

813 Schmidt-Kloiber, A., & Hering, D. (2015). www.freshwaterecology.info – An online tool that

814 unifies, standardises and codifies more than 20,000 European freshwater organisms

815 and their ecological preferences. *Ecological Indicators*, *53*, 271–282.

816 https://doi.org/10.1016/j.ecolind.2015.02.007

817 Shumilova, O., Tockner, K., Thieme, M., Koska, A., & Zarfl, C. (2018). Global Water

818 Transfer Megaprojects: A Potential Solution for the Water-Food-Energy Nexus?

819 *Frontiers in Environmental Science*, *6*. https://doi.org/10.3389/fenvs.2018.00150

820 Skøien, J. O., Merz, R., & Blöschl, G. (2006). Top-kriging - geostatistics on stream networks.

821 *Hydrology and Earth System Sciences*, *10*(2), 277–287. https://doi.org/10.5194/hess-

822 10-277-2006

823 Snelder, T. H., & Booker, D. J. (2013). Natural Flow Regime Classifications Are Sensitive to

824 Definition Procedures. *River Research and Applications*, *29*(7), 822–838.

825 https://doi.org/10.1002/rra.2581

826 Strayer, D. L., & Dudgeon, D. (2010). Freshwater biodiversity conservation: recent progress

827 and future challenges. *Journal of the North American Benthological Society*, *29*(1),

828   344–358. https://doi.org/10.1899/08-171.1

829   Tennant, D. L. (1976). Instream Flow Regimens for Fish, Wildlife, Recreation and Related

830   Environmental Resources. *Fisheries*, *1*(4), 6–10. https://doi.org/10.1577/1548-

831   8446(1976)001<0006:IFRFFW>2.0.CO;2

832   Tickner, D., Opperman, J. J., Abell, R., Acreman, M., Arthington, A. H., Bunn, S. E., et al.

833   (2020). Bending the Curve of Global Freshwater Biodiversity Loss: An Emergency

834   Recovery Plan. *BioScience*, *70*(4), 330–342. https://doi.org/10.1093/biosci/biaa002

835   Tonkin, J. D., Poff, N. L., Bond, N. R., Horne, A., Merritt, D. M., Reynolds, L. V., et al.

836   (2019). Prepare river ecosystems for an uncertain future. *Nature*, *570*(7761), 301–303.

837   https://doi.org/10.1038/d41586-019-01877-1

838   Ver Hoef, J. M., & Peterson, E. E. (2010). A Moving Average Approach for Spatial

839   Statistical Models of Stream Networks. *Journal of the American Statistical*

840   *Association*, *105*(489), 6–18. https://doi.org/10.1198/jasa.2009.ap08248

841   Ver Hoef, J. M., Peterson, E. E., Clifford, D., & Shah, R. (2014). SSN : An R Package for

842   Spatial Statistical Modeling on Stream Networks. *Journal of Statistical Software*,

843   *56*(3). https://doi.org/10.18637/jss.v056.i03

844   Vigiak, O., Lutz, S., Mentzafou, A., Chiogna, G., Tuo, Y., Majone, B., et al. (2018).

845   Uncertainty of modelled flow regime for flow-ecological assessment in Southern

846   Europe. *Science of The Total Environment*, *615*, 1028–1047.

847   https://doi.org/10.1016/j.scitotenv.2017.09.295

848   Warton, D. I., & Hui, F. K. C. (2011). The arcsine is asinine: the analysis of proportions in

849   ecology. *Ecology*, *92*(1), 3–10. https://doi.org/10.1890/10-0340.1

850   Zarfl, C., Lumsdon, A. E., Berlekamp, J., Tydecks, L., & Tockner, K. (2015). A global boom

851   in hydropower dam construction. *Aquatic Sciences*, *77*(1), 161–170.

852   https://doi.org/10.1007/s00027-014-0377-0

853   Zimmerman, D. L., & Ver Hoef, J. M. (2017). The Torgegram for Fluvial Variography:

854   Characterizing Spatial Dependence on Stream Networks. *Journal of Computational*

855   *and Graphical Statistics*, *26*(2), 253–264.

856   https://doi.org/10.1080/10618600.2016.1247006

857   Zolezzi, G., Bellin, A., Bruno, M. C., Maiolini, B., & Siviglia, A. (2009). Assessing

858   hydrological alterations at multiple temporal scales: Adige River, Italy. *Water*

859   *Resources Research*, *45*(12). https://doi.org/10.1029/2008WR007266

860

Tables

Table 1 - List of the IHA flow metrics adopted in the analyses as computed from the 23 years simulated streamflow time series

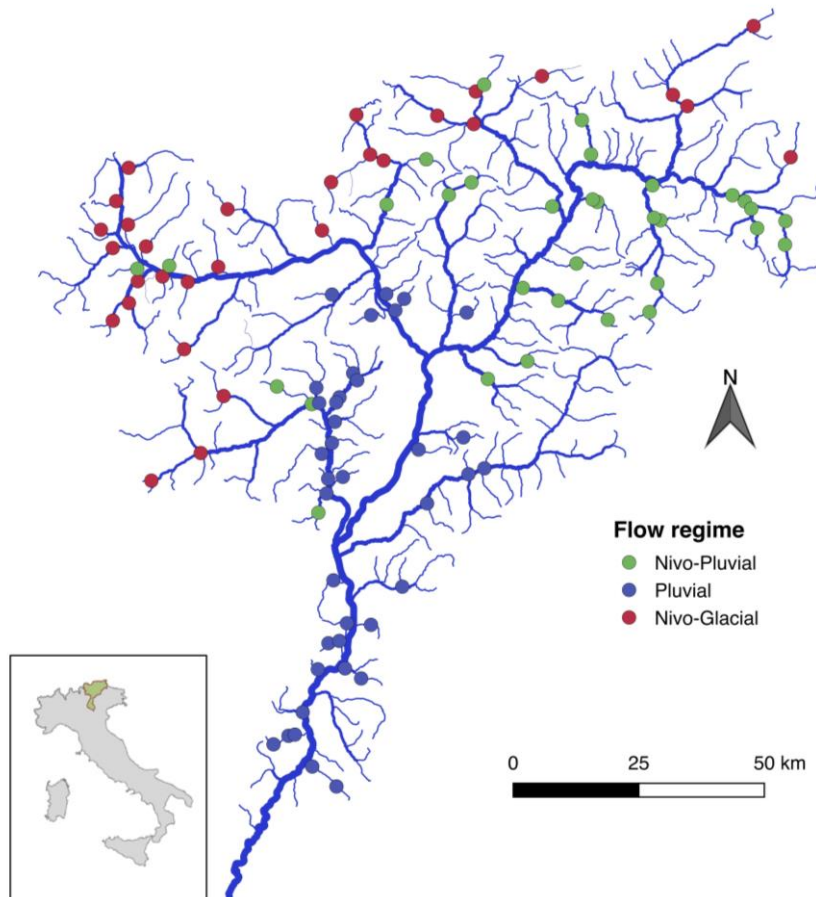| Flow component	IHA flow metric name	Description
Magnitude of monthly flow conditions (12 parameters)	January, February, March, April, May June, July, August, September, October, November, December	Mean flow for January, …, December
Magnitude and duration of extreme conditions (11 parameters)	1, 3, 7, 30, 90 Day Min 1, 3, 7, 30, 90 Day Max Base index	Minimum flow, 1, 3, 7, 30, 90 day mean Maximum flow, 1, 3, 7, 30, 90 day mean 7 days minimum / mean flow
Timing of extreme flow conditions (2 parameters)	min Julian max Julian	Mean Julian data of annual 1-day maximum Mean Julian data of annual 1-day minimum
Frequency and duration of high and low pulses (4 parameters)	Low pulse number High pulse number Low pulse length High pulse length	Number of flow events below 25th percentile Number of flow events above 75th percentile Number of days below 25th percentile Number of days above 75th percentile
Rate of change and variation (5 parameters)	Rise rate Fall rate Reversals y.CV m.CV	Median of all positive differences between consecutive values Median of all negative differences between consecutive values Number of times flow period switches from rising to falling and vice-versa Average annual coefficient of variation (SD/mean) Average monthly coefficient of variation (SD/mean)

881   **Table 2-** Loadings of the flow metrics on the first two axes of the PCA within each

882   hydrologic class. Metrics presenting high correlation with the axes (>0.8) are highlighted in

883   bold. Codes of the IHA parameters described in Table 1.

884

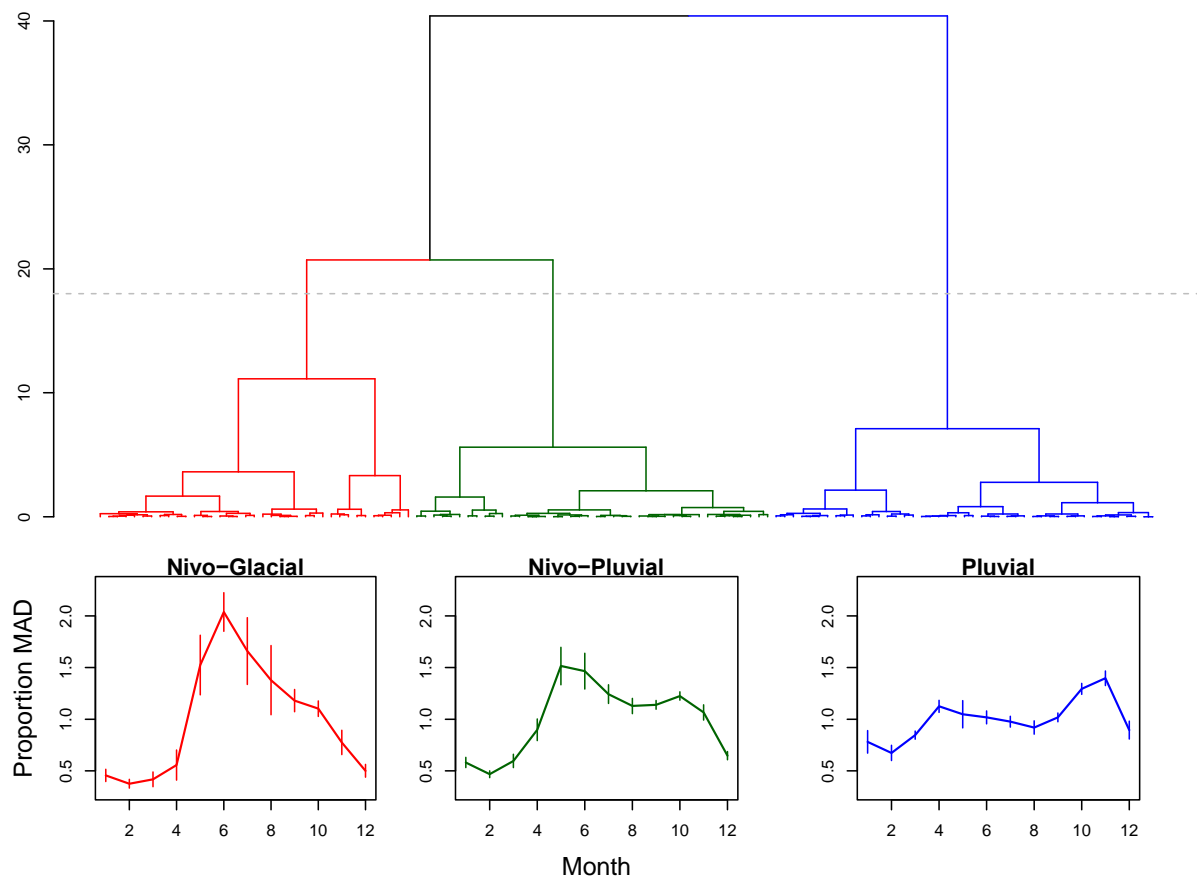| IHA parameter	Glacial		Pluvial-nival		Pluvial	
	Axis1	Axis2	Axis1	Axis2	Axis1	Axis2
January	**-0.94**	-0.16	**-0.96**	0.00	-0.73	0.60
February	**-0.96**	-0.15	**-0.89**	-0.23	**-0.81**	0.56
March	**-0.96**	-0.12	**-0.80**	-0.47	-0.65	0.46
April	**-0.90**	-0.10	-0.75	-0.55	0.24	-0.24
May	**-0.83**	0.25	**0.86**	-0.13	0.21	**-0.86**
June	0.42	0.49	0.68	0.53	-0.11	**-0.93**
July	**0.93**	-0.17	-0.22	**0.92**	-0.41	-0.74
August	**0.90**	-0.33	-0.46	0.78	-0.03	-0.74
September	**0.82**	-0.50	-0.58	0.70	-0.22	-0.64
October	**-0.85**	-0.19	-0.80	0.01	-0.34	0.35
November	**-0.98**	0.01	-0.79	-0.51	-0.59	0.72
December	**-0.97**	-0.12	**-0.91**	-0.26	-0.71	0.68
1 Day Min	**-0.98**	-0.14	**-0.98**	0.02	**-0.99**	0.08
1 Day Max	-0.20	**0.96**	0.77	-0.59	**0.91**	0.32
3 Day Min	**-0.98**	-0.14	**-0.98**	0.00	**-0.99**	0.09
3 Day Max	-0.25	**0.92**	0.78	-0.58	**0.90**	0.35
7 Day Min	**-0.98**	-0.14	**-0.98**	-0.02	**-0.98**	0.13
7 Day Max	-0.23	**0.85**	0.80	-0.55	**0.91**	0.36
30 Day Min	**-0.98**	-0.14	**-0.96**	-0.12	**-0.94**	0.31
30 Day Max	0.12	0.76	**0.90**	-0.36	**0.96**	0.22
90 Day Min	**-0.99**	-0.11	**-0.90**	-0.40	**-0.87**	0.46
90 Day Max	**0.92**	0.22	**0.98**	0.00	**0.97**	0.11
Base index	**-0.98**	-0.14	**-0.98**	-0.02	**-0.98**	0.13
min_julian	0.77	-0.04	0.71	0.45	0.41	0.38
max_julian	-0.12	0.13	**-0.81**	-0.32	-0.79	0.41
High pulse length	-0.44	-0.40	0.22	0.18	-0.24	-0.32
High pulse number	0.58	0.07	-0.47	-0.29	0.27	0.52
Low pulse length	0.58	-0.15	0.06	**0.94**	-0.55	-0.63
Low pulse number	-0.48	0.16	-0.20	-0.92	0.18	**0.92**
Rise rate	0.72	0.24	0.71	-0.40	0.77	0.46
Fall rate	**0.91**	-0.07	0.39	**0.80**	-0.61	-0.64
Reversals	0.61	0.04	-0.25	-0.52	0.67	0.12
m.CV	-0.38	0.75	0.65	-0.74	**0.92**	0.38
y.CV	-0.39	0.54	0.48	**-0.82**	**0.88**	-0.01

885

886

887

888

889

890

891

893 **Table 3-** Parameters of the spatial stream-network models that performed better with respect

894 to the RMSPE metric for each flow-regime. The covariates (predictors) selected in the model,

895 the associated sign of effect, and the proportion of variance explained by the covariates and

896 spatial autocorrelation are listed for each response variable. The asterisk indicates the

897 presence of a significant term (at a significance $\alpha < 0.05$) in the model. Principal Components

898 for the three flow regimes are defined as PC.iha.gl, PC.iha.pn and PC.iha.pl, for the nivo-

899 glacial, nivo-pluvial and pluvial streams, respectively.

900

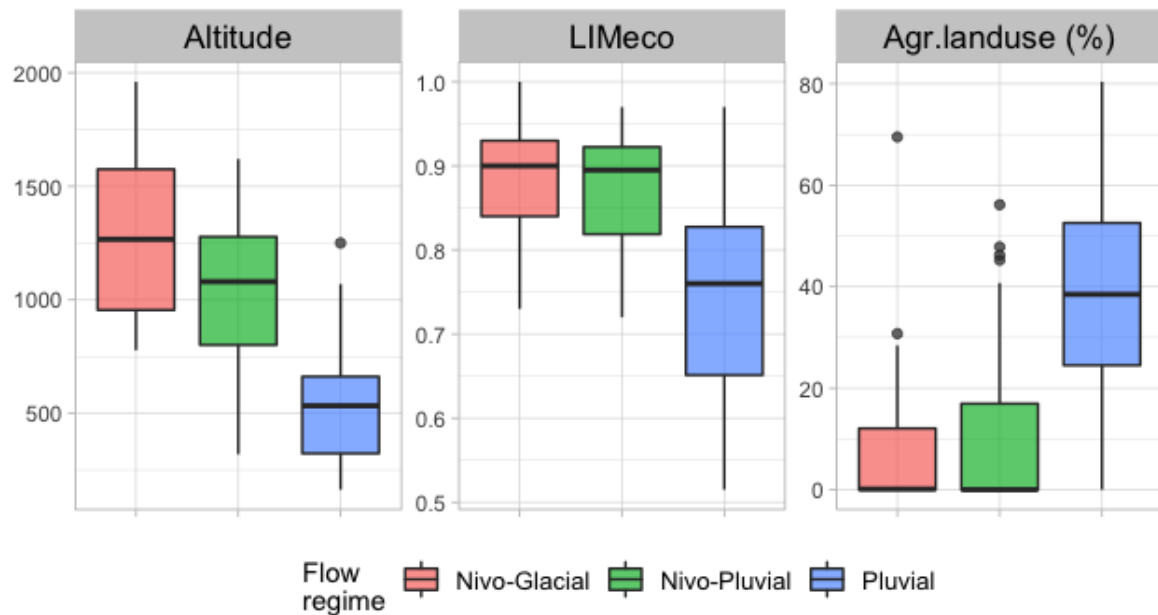| Response variable	Nivo-Glacial			Nivo-Pluvial			Pluvial		
	Selected covariates	Proportion of variance		Selected covariates	Proportion of variance		Selected covariates	Proportion of variance	
		Covariate	*Spatial*		*Covariate*	*Spatial*		*Covariate*	*Spatial*
Richness	PC1.iha.ng(-) Limeco (+) Agr.landuse (-)*	0.28	0.71	PC1.iha.np (+) Agr.landuse (-)	0.14	0.66	PC1.iha.pl (+)* Limeco (+)	0.16	0.35
Shannon	Limeco (+)* Agr.landuse (-)	0.21	0.77	Limeco (+)*	0.14	0.72	Agr.landuse (-) Limeco (+)*	0.33	0.67
Fdis	Limeco (+)	0.1	0.18	PC1.iha.np (-) Limeco (-)	0.13	0.52	PC2.iha.pl (-)* Limeco (+)	0.2	0.63
Star_ICMi	Agr.landuse (-)*	0.28	0.13	PC1.iha.np (+)	0.1	0.88	Limeco (+)*	0.3	0.53
Grazers	PC1.iha.ng (-)* PC2.iha.ng (+)	0.19	0.47	PC1.iha.np (+) Agr.landuse (+)	0.02	0.89	PC2.iha.pl (+)	0.09	0.42
Shredders	Agr.landuse (-)	0.11	0.81	Limeco (+) Agr.landuse (-)	0.18	0.81	Limeco (+)*	0.52	0.45
Gatherers	PC1.iha.ng (-)	0.07	0.62	Agr.landuse (-)	0.03	0.95	PC1.iha.pl (-)* PC2.iha.pl (+) Limeco (-)	0.23	0.76
Filterers	PC1.iha.ng (+)	0.01	0.9	Agr.landuse (+)	0.01	0.93	PC1.iha.pl (+)*	0.12	0.32
Predators	Limeco (+)	0.11	0.34	Agr.landuse (-)	0.09	0.91	Limeco (+)*	0.22	0.78
Small size	PC1.iha.ng (-)*	0.12	0.85	PC1.iha.np (+)*	0.21	0.78	Agr.landuse (-)*	0.13	0.45
Large size	PC1.iha.ng (+)* Limeco (-)	0.17	0.82	PC2.iha.np (+)*	0.15	0.78	Agr.landuse (-)*	0.19	0.7

901

902

903

904

905

906

Figures

Figure 1 - Map of the Adige River network showing the locations of the 100 biological monitoring sites for which 25 years of natural streamflow time series were simulated. Colours define the distribution of the three identified flow regime classes (see Sect. 2.4).
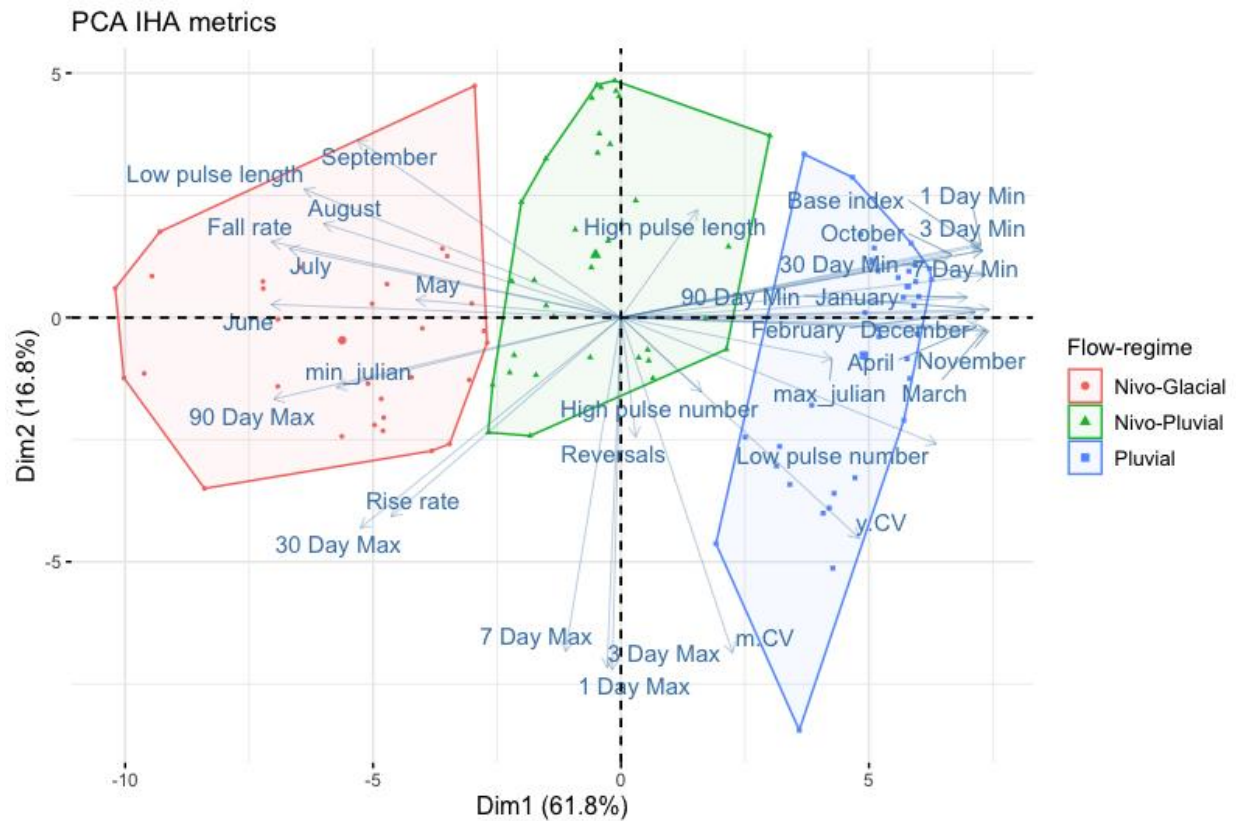
922

923

924

925

926

927

Figure 2 - Dendrogram of the study reaches based on flexible beta-clustering of the first two
weighted Principal Components (explaining 92% of variation) of the MAD-normalised
monthly hydrographs. Lower panels show the mean across sites (± SD) of normalised
hydrographs (as proportion of mean annual discharge; MAD) for each identified streamflow
regime class.

933

934

935

936

937

938

939

940

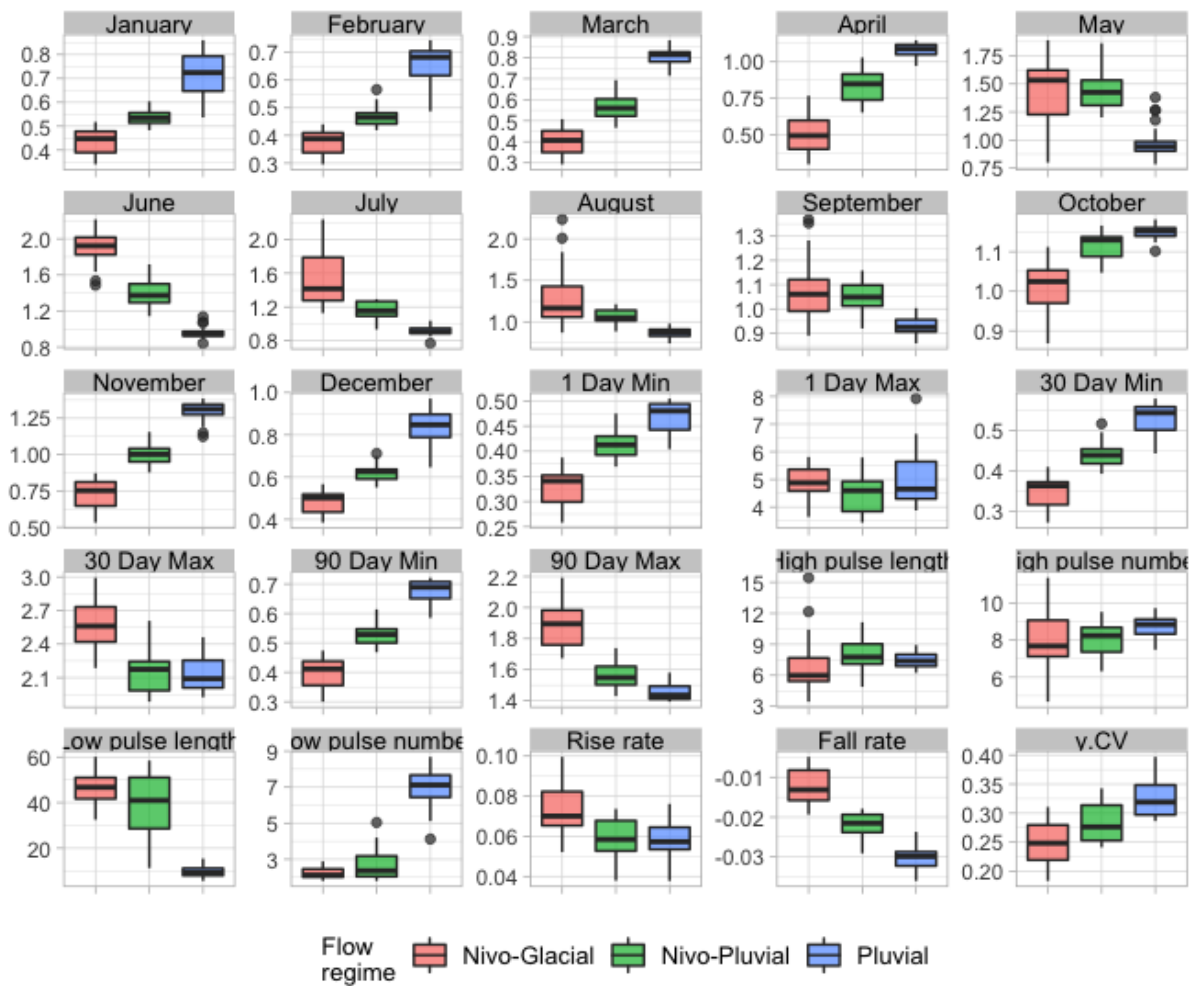Figure 3- Boxplot of selected environmental descriptors for each identified streamflow regime class. The following boxplot representation is adopted: line for median; box for the inter-quartile range; whiskers for 1.5 times the inter-quartile range; dots for the outliers.

945

946

947

948

949

950

951

952

953

954

955

956

957

PCA IHA metrics

Figure 4 - Biplot of the PCA based on 34 IHA flow metrics (direction and loading indicated by the blue arrows) derived from the 23 years streamflow series for the 100 investigated study sites. The sites are grouped according to the streamflow regime class previously determined by the flexible beta-clustering approach.

968

969

970

971

972

973

974

975

976

977

978 **Figure 5** - Boxplot of selected IHA streamflow metrics aggregated for each identified flow

979 regime class.

980

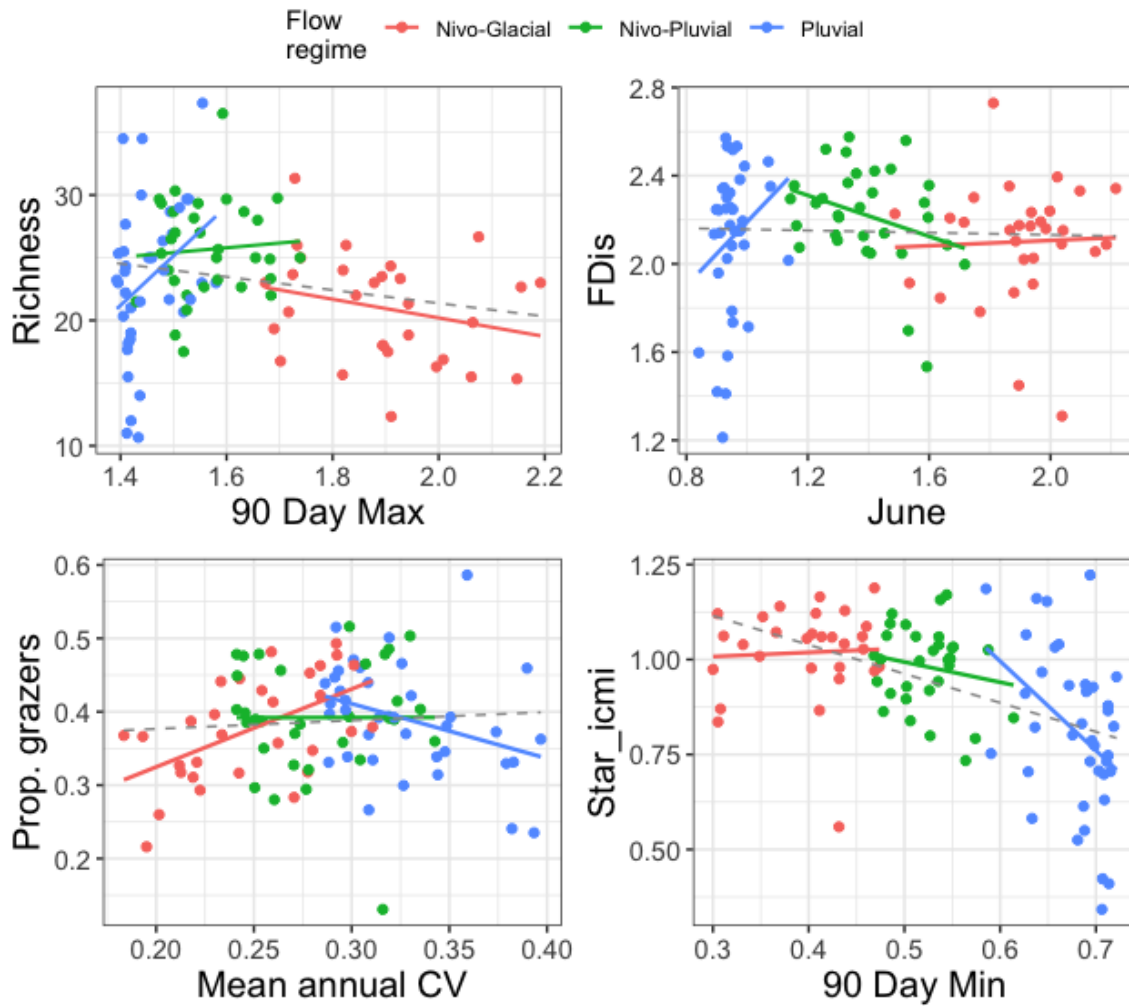981

982

983

984

985

986

987   Fig 6. Illustrative examples of variable flow-ecology relationships among the three identified

988   streamflow regimes. The dashed grey line shows the overall relationship observed combining

989   the three flow-regimes. Note that the fits between flow and biotic metrics in each flow-

990   regime are only shown for exemplifying purposes. The full set of flow-ecology relationships

991   from the SSN models are reported in Tab.3.

992

993

994

995

996

997

998

999

1000
1001
1002
1003